

On the delay between water temperature and invertebrate community response to warming climate

Valeria Lencioni, Elisa Stella, Maria Grazia Zanoni, Alberto Bellin



PII: S0048-9697(22)02856-X

DOI: <https://doi.org/10.1016/j.scitotenv.2022.155759>

Reference: STOTEN 155759

To appear in: *Science of the Total Environment*

Received date: 13 January 2022

Revised date: 2 April 2022

Accepted date: 3 May 2022

Please cite this article as: V. Lencioni, E. Stella, M.G. Zanoni, et al., On the delay between water temperature and invertebrate community response to warming climate, *Science of the Total Environment* (2021), <https://doi.org/10.1016/j.scitotenv.2022.155759>

This is a PDF file of an article that has undergone enhancements after acceptance, such as the addition of a cover page and metadata, and formatting for readability, but it is not yet the definitive version of record. This version will undergo additional copyediting, typesetting and review before it is published in its final form, but we are providing this version to give early visibility of the article. Please note that, during the production process, errors may be discovered which could affect the content, and all legal disclaimers that apply to the journal pertain.

On the delay between water temperature and invertebrate community response to warming climate

Valeria Lencioni^{a,*}, Elisa Stella^b, Maria Grazia Zanoni^c, Alberto Bellin^c

^a *Climate and Ecology Unit, Research and Museum Collection Office, MUSE-Museo delle Scienze,
Corso del Lavoro e della Scienza 3, Trento, 38122, Italy,*

^b *Department of Environmental Sciences, Informatics and Statistics, Ca' Foscari University of
Venice, Scientific Campus, Via Torino, 155, Mestre-Venice, 30172, Italy,*

^c *Department of Civil, Environmental and Mechanical Engineering, DICAM, University of Trento,
Via Mesiano, 77, Trento, 38123, Italy,*

Abstract

We evaluated the effect of global warming on invertebrate communities at high altitudes using data from the Careser system. We procured data on air temperature, which was obtained over 50 years at altitudes above 2600 m a.s.l., and data on water temperature, which was available for approximately 30 years. We sampled thrice in the past 20 years (2001, 2014, 2018) at three sampling sites (CR0-meta-kryal, CR1-hypokryal, CR2-glacio-rhithral) of the Careser glacier-fed stream and its main non-glacial tributary (CR1bis-krenal). Warmer climates were observed in the last decade compared to the 1980s, with a mean maximum summer air temperature (mTmax) increase of 1.7 °C at 2642 m a.s.l. and 1.8 °C at 2858 m a.s.l. Compared to air temperatures, the rise in water temperature was delayed by approximately 20 years; water mTmax started to increase

* Corresponding author

Email address: Valeria.Lencioni@muse.it (Valeria Lencioni)

in 2003, reaching 8.1 °C at 2642 m a.s.l. and 2.4 °C at 2858 m a.s.l in the year 2020. The invertebrate community exhibited a delayed response approximately 13 years from the water warming; there was a sequential increase in the number of taxa, Shannon diversity, and after 17 years, functional diversity. In the kryal sites, taxonomical and functional diversity changed more consistently than in the glacio-rhithral site in the same period, due to the arrival of taxa that were previously absent upstream and bearers of entirely new traits. Progressive taxonomical homogenisation was evident with decreasing glacial influence, mainly between glacio-rhithral and krenal sites. The numbers of *Diamesa steinboecki*, an insect that was adapted to the cold, declined in summer (water mTmax > 6 °C and air mTmax > 12 °C). This study highlights the mode and time of response of stream invertebrate communities to global warming in alpine streams and provides guidelines for analysing changes in the stream invertebrate communities of other glacial systems in alpine regions.

Keywords: water temperature, glacier-fed streams, chironomids, community structure, functional diversity, Italian Alps

1. Introduction

In recent decades, mountain glaciers have retreated and thinned dramatically as a result of global warming (Zemp et al., 2015). In addition to glacial melting, which proceeds at a relentless pace, winter snow accumulation has been declining in both glacial and non-glacial areas (Matiu et al., 2021), leading to cascade effects on river ecosystems. In the European Alps, 76-97% of the actual glacier volume is predicted to disappear within the XXI century (Beniston et al., 2018), and small glaciers with area < 0.5 km² are expected to disappear within a few decades (Huss and Fischer, 2016; Zemp et al., 2015). These changes affect the hydrological and thermal regimes

(Kaser et al., 2010; Immerzeel et al., 2020; Niedrist and Füreder, 2021) and the bio-geochemical cycles, and in turn, the aquatic communities (Milner et al., 2017) of glacial-fed rivers. Therefore, these rivers can serve as model systems for investigating the effects of climate change on mountain ecosystems because of their strong atmosphere–cryosphere links, rich biodiversity (Gobbi and Lencioni, 2020), and significant conservation interest concerning the habitat *sensu stricto* and endemic species under the threat of extinction (Fell et al., 2017; Gobbi et al., 2021).

Many studies have analysed how climate change affects glacier dynamics and the streamflow of glacier-fed streams at a multiplicity of spatial scales (see, for example, Chen and Ohmura, 1990; Brown et al., 2006). The general picture is that the first glacier runoff increases due to temperature rise, attains a maximum, and declines when the glacial area contributing to the runoff decreases due to glacier thinning (Cauvy-Frami   et al., 2016; Brighenti et al., 2019). Several alpine catchments have already crossed this hydrological tipping point of maximum summer discharge associated with glacier disappearance (Huss and Hock, 2018).

As the atmospheric temperature continues to rise globally (IPCC, 2018) and glacial runoff decreases, the water temperature will adjust to the local air temperature rise, with incremental warming during the summer (Milner et al., 2001; Webb et al., 2008; van Vliet et al., 2011; Niedrist and F  reder, 2021). Water temperature has been recognised as the major controlling factor of the biological, chemical, and physical conditions of freshwater ecosystems (Caissie, 2006; Webb et al., 2008) and is the most important environmental variable influencing invertebrate communities in mountain streams (Milner et al., 2001; Dickson et al., 2012; Lencioni et al., 2015). Owing to the rise in water temperature, the composition and functional characteristics of these communities have changed in alpine settings that have been significantly transformed by climate change (Brown et al., 2018). Cold stenothermal species could undergo extinction, and are expected to be

replaced by eurythermal and euriecious species, which are bearers of new functional traits in the kryal sectors (Hotaling et al., 2017; Brown et al., 2018; Bruno et al., 2019). Specifically, the functional traits of organisms are central to understanding the processes maintaining biodiversity because organisms respond consistently to environmental gradients; thus, they are of particular interest in studying the effects of climate change (Poff, 1997).

In this study, we analysed how the water temperature and fauna of a glacier-fed river responded to the rapid retreat of the feeding glacier due to global warming. We expect that with declining environmental stress (i.e. decreasing glacial influence and increasing water temperature), in a less extreme environment, the influence of niche complementarity on species fitness would increase, while that of environmental filtering would decrease (Mason et al., 2013). In this study, we have hypothesised that faunal changes were not simultaneous with environmental changes. Specifically, the hypotheses were (i) water temperature has been increasing with a delay and to a lesser extent than air temperature due to various factors such as the higher heat capacity of water compared to air, and the evaporation and cold ice-melt inputs that moderate the air warming effect (Webb et al., 2003); (ii) invertebrate community structure and function have been changing, but with a delay with respect to rising water temperature because glacier-fed invertebrates show plasticity of key fitness-associated traits, such as reproductive performance (Füreder and Niedrist, 2020), thereby increasing their resilience. In fact, invertebrates may face initial water warming through physiological or behavioural adaptation within the upper thermal limit. Beyond this limit, invertebrates respond to new environmental conditions with genetic adaptation, migration, or extinction depending on species-specific vulnerability (Calow, 1989). With this study we wanted to find this limit for water temperature.

2. Material and Methods

2.1. Study area

The study area was located within the Stelvio National Park in the Rhaetian Alps NE of Italy (46 ° N, 9-10 ° E; Trentino Province), and belonged to the Ortles-Cevedale chain (Figure 1). Within this area, four study sites were identified: three along the main stem of the Careser stream, fed by the Careser glacier (CR0, CR1, CR2), and one on its main non-glacial tributary (CR1bis) (Table 1 and Figure 1). The Careser glacier, feeding the stream, has an area of 1.4 km² (Smiraglia and Diolaiuti, 2015) and has been retreating at a rate of 21.7 m a y⁻¹ since the end of the last century (Casarotto and Bertoni, 2015). The Careser glacier lost 79% (-5.2 km²) of its surface area from the end of the Little Ice Age and has been losing 2.3% of its surface area per year since 1987 (Carturan et al., 2013). All sites were located above the treeline (> 2000 m a.s.l.), within 2.3 km downstream from the source, along a restricted glacial influence gradient estimated using the glacial index (GI) and the percentage of glacier cover in the catchment (GCC), according to Jacobsen and Dangles (2012) for glacial sites: $GI = 0.32-0.61$ and $GCC = 33-51\%$ (Lencioni et al., 2021). The four study sites belonged to three habitat types reflecting the stream origin on which they were chosen: klyal (CR0, CR1), glacio-rhithral (CR2), and kreno-rhithral (CR1bis), as shown in Table 1, according to the Castella et al. (2001) classification. The geomorphological, hydrological, physical, and chemical parameters of the four study sites are available in Lencioni et al. (2021) and Debiasi et al. (2022), and their main physicochemical features are summarised in Table S1 of the Supplementary Material (SM). All sites were sampled during the ice-free period, in July and September, between 2001 and 2018: CR1, CR2, and CR1bis in 2001; CR0 and CR2 in 2014, and all sites in 2018.

2.2. Temperature data

We considered the maximum air temperature to be the main driver of changes in water temperature (Tlhalerwa and Mphale, 2021). The time series (from 1971 to 2020) of the measured daily maximum air temperature were obtained from the Meteorological Offices of Trento (Meteotrentino, <http://www.meteotrentino.it>) and Bolzano (<http://www.provincia.bz.it/meteo/home.as>) provinces, and the Austrian weather service (ZAMG, <http://www.zamg.ac.at>) at the 32 meteorological stations closer to the above study sites and at elevations above 2000 m a.s.l (above sea level). The time series were then inspected for outliers, and a few temperature measurements larger than 30 °C were eliminated because they were clearly affected by instrumental errors. The measured daily maximum air temperatures were then interpolated at the investigated sites using Kriging with an external drift (KED) with the terrain elevation as a secondary variable (Goovaerts, 1997) and using the following exponential isotropic covariance function with:

$$C(r) = \begin{cases} \sigma_g^2 + \sigma^2 \exp\left[-\frac{r}{I}\right], & r = 0 \\ \sigma^2 \exp\left[-\frac{r}{I}\right], & r > 0 \end{cases} \quad (1)$$

where r is the two-point separation distance (i.e. the distance between the two points with respect to which the covariance is computed), σ_g^2 is the variance of the nugget effect, representing uncaptured variability at scales smaller than the minimum distance between the meteorological stations, σ^2 is the temperature variance, and I is the integral scale, which reflects the spatial pattern. Because the time series are discontinuous, interpolation was performed by eliminating the meteorological stations lacking the measured temperature at each time step. The optimal values of these parameters were obtained by minimising the difference between T_{max} measured at the

Careser dam meteorological station (see Figure 1) and the interpolated values at the same location. We excluded the Careser dam from the 32 meteorological stations used for interpolation, and obtained the interpolated values by applying the KED. The optimised parameters were as follows: $\sigma_g^2 = 39.02(^{\circ}C)^2$, $\sigma^2 = 16.26(^{\circ}C)^2$, and $I = 5605m$, and were used in the KED algorithm to obtain the maximum temperature distribution at the four study sites (CR0, CR1, CR1bis, and CR2). In contrast to the computation of the optimal covariance parameters, the Careser Dam meteorological station was included in the 32 stations used for interpolation.

Water temperature was measured at 1-hour intervals with digital loggers (Onset Hobo TidbiT®, Escort Junior, TinyTag, and TinyTalk) by the Meteorological Office of the Provinces of Trento (Meteotrentino, <http://www.meteotrentino.it>) and by the MUSE-Science Museum of Trento at the following time intervals: 1992÷1993, 2000÷2003, 2010 and 2014÷2019 for CR2; 2001÷2003 and 2010 for CR1; 2010 and 2014÷2019 for CR0; 2001÷2003 and 2018÷2020 for CR1bis. The 2010 data refer to the period July-October and have been obtained from an experimental temperature sensor deployment performed in collaboration with Meteotrentino and Matthew Becker of the California State University, Long Beach (see the acknowledgments).

The measured water temperature data were employed in a neural network (NN) model, with the air temperature data interpolated using KED, to reconstruct the missing water temperature values at each site.

2.3. *Invertebrate sampling and identification*

At each study site, benthic invertebrates were collected three times/year in 2001, 2014 and 2018 during summer by kick sampling of $5 \times 0.1 m^2$ area (five replicates) within a reach of 15 m

in length, according to Castella et al. (2001). In all, 135 replicates were collected. The 15 m-long reaches were defined to represent the different sectors identified on the basis of valley and channel geomorphology. The first reach was as close to the glacier snout as possible (CR1 in 2001 and CR0 after 2014). The second reach was within 1000 m of the glacier and upstream of any major tributary input (CR1 in 2018). The lowest site was selected where a fully developed macroinvertebrate community occurred, that is, where Chironomidae were at least codominant with EPT (Ephemeroptera, Plecoptera, and Trichoptera) (CR2 in all years). This downstream limit also represents the last stream sector upstream of the reservoir. The replicates were taken from all microhabitat types (riffles, pools, etc.), proportionally to their frequency in the 15 m reach. A $33 \times 33 \text{ cm}$ pond net with a $100 \mu\text{m}$ mesh was used for sampling this site. The samples were washed through a $100 \mu\text{m}$ mesh funnel to remove excess water and preserved in a solution of 75% ethanol. Specimens were identified to the genus or species level (Diptera Chironomidae, Ephemeroptera, and Plecoptera) or higher taxonomic levels (other Diptera, Coleoptera, Trichoptera, Oligochaeta, Nematoda, Tricladida, Crustacea, and Hydracarina). All specimens (in 75% ethanol and on microscope slides) were deposited in the MUSE-Museo delle Scienze of Trento (Italy) for archiving in the collection cINV0017.

During sorting under a stereomicroscope (50X), coarse particulate organic matter (BPOM) was separated from each benthic replicate, dried at 60°C for 1 h, and ashed at 500°C for 1 h in a muffle furnace. The BPOM results are presented in Table S1. Nine sampling units were considered (site \times year).

Biomass (wet weight, mg) was added to each taxon. Values were considered as mean wet weight referred to the last aquatic instar of each taxon, based on data from previous studies (Brighenti et al., 2021, for example) and from the data for this study (mean wet weight of 50

IV-instar larvae/species, (Lencioni, 2000) (Table S2).

2.4. *Functional traits*

The functional features of invertebrate communities were characterised using 10 biological traits (29 states or modalities) describing life history (body size, number of cycles per year, pupation, and adult life stages), resilience or resistance potentials (locomotion/substrate attachment, resistance forms), and physiology (respiration mode, feeding habit, and temperature preference) (Table 2), (Poff et al., 2006; Brown et al., 2018; Bruno et al., 2019; Tachet et al., 2010). These traits were selected to provide information on phenotypic responses that have been previously suggested as indicators of environmental changes in localised studies of glacier-fed river invertebrate communities (Ilg and Castella, 2006; Brown et al., 2018). We avoided ecological traits that described habitat preferences, as these typically represented the ‘outcome’ of biological traits according to Brown et al. (2018). With regard to traits associated with the life cycle, UNIV refers to species which, depending on the yearly weather conditions (e.g. cold and snowy winters, period of onset of glacial melting), can be uni- or bivoltine (this has been observed in species of *Diamesa*). In addition, an ecological trait called “glacial affinity” was also analysed to track potential changes in taxa that were restricted, frequent, or absent in glacier-fed streams. Each taxon was coded according to its affinity for each trait category using a fuzzy coding approach (Chevenet et al., 1994). Fuzzy coding data were then converted to percentages of affinity for each trait. This procedure standardises the potential differences in the codification scores (i.e. different row sums for each taxon and trait). Specifically, we defined fuzzy codes (0 = no affinity, 1 = weak affinity, 2 = medium affinity, 3 = strong affinity) for the ten traits.

2.5. Data analysis

2.5.1. Modelling water temperature

The daily maximum water temperature was reconstructed for the period 1971÷2020 for CR2, and 1990÷2020 for the other sites, because water temperature data were available since 1990 for the former and since 1992 for the other sites. For this purpose, we trained a multi-layer perceptron neural network (MLP NN) to the available daily water temperature data, such as filling the gaps at CR1bis, CR2, and CR1 and simulating the entire time series at CR0, for which no reliable measurements were available.

For CR1, we also used the water temperature measured at CR2 to train the MLP NN to compensate for the relatively small amount of available data at this site. Similarly, for CR0, the water temperature measurements at both CR2 and CR1 were included in the training set, while the measurements of CR0 were employed for comparison with the values predicted using the model. The output values of the MLP NN model were the water temperature time series of the considered sites, while the input values (features) were the Julian day and year of the measurements and the interpolated air temperature at the sampling site obtained using KED, as described in Section 2.2. In addition, for the modelling of the CR1 and CR0 time-series, the coordinates and elevation were also included as features, because different stations were implemented in the prediction.

We used an MLP NN with two hidden layers, with each layer comprising 10 units, and the rectified linear unit (ReLU) as the activation function (Goodfellow et al., 2016; Glorot et al., 2011), which can be mathematically described as the maximum function over the set of 0 and the input value:

$$g(z) = \max(0, z) \quad (2)$$

The parameters of the MLP NN were obtained by minimising the Mean Squared Error

index as a loss function:

$$MSE = \frac{1}{N} \sum_{i=1}^N [y_{pred,i} - y_{meas,i}]^2 \quad (3)$$

where $y_{meas,i}$ and $y_{pred,i}$ are the measured and predicted values, respectively, and N is the number of samples.

Owing to the limited amount of available data, the 30-fold cross-validation procedure (Raschka, 2015) was applied by randomly splitting the dataset into 30 groups. Each group was used as a test set with the remaining 29 groups as the training set, on which the model was trained by minimising MSE (3). At the end of each training step, the model was compared with the test set and the Nash-Sutcliffe index computed as a quality index:

$$NSE = 1 - \frac{\sigma_e^2}{\sigma_o^2} \quad (4)$$

where σ_e^2 is the variance of the error, and σ_o^2 is the variance of the measurements. The mean of the 30 cross-validation NSF values were 0.85, 0.94, 0.84, and 0.81 for CR2, CR1bis, CR1, and CR0, respectively.

Finally, following Raschka (2015), the models were trained for the last time on the entire dataset of the available data, for each site, the parameters learned in this phase were employed to predict the complete time series of the locations. The NSE values, obtained considering the complete training set, confirmed the levels of accuracy achieved in the cross-validation phase and they were: 0.86, 0.94, 0.83 and 0.82 for CR2, CR1bis, CR1 and CR0, respectively.

The main architecture of the MLP NN model was implemented using the *Keras* deep-learning library (Chollet, 2018) and for the cross-validation procedure, the *scikit-learn* package was used (Pedregosa et al., 2011), both of which were developed in Python.

2.5.2. *The community structure: taxonomic diversity and biomass*

Seventy-three taxa were identified in this study. The sum of their abundance values in replicates expressed per square meter (ind m^{-2}) per site/year (i.e. pooling replicates per year) was considered for a total of nine sampling units. The diversity (alpha and beta) of invertebrate communities was analysed at the specified site and year of sampling. Alpha diversity was estimated as the number of species (S) = local taxon richness, population density ($N = \text{ind m}^{-2}$), and diversity using the Shannon-Wiener index (H) (Shannon and Weaver, 1949).

Beta diversity was calculated using the Bray-Curtis dissimilarity (Bray and Curtis, 1957). To analyse which species contributed the most to beta diversity, we performed the SIMPER analysis (Clarke, 1993), with the abundance data normalised by its maximum value for each community. The SIMPER analysis was conducted by performing pairwise comparisons of groups of sampling units to identify the average contributions of each species to the average overall Bray-Curtis dissimilarity. This function displays the most important species for each pair of groups. Software R, version 4.0.3, was used to calculate taxonomic diversity. The Bray-Curtis dissimilarity and SIMPER analyses were performed using the *vegan* package, implemented in R.

In addition, the total biomass within the communities was computed by multiplying the number of individuals with their respective weights. The logarithm of its distribution in the four sampling units was plotted using a violin plot, which has an advantage over the box plot, to show the sample probability distribution function.

2.5.3. *The community structure: functional diversity*

Changes in functional diversity in space and time were assessed using the two-sample Kolmogorov-Smirnov (KS) test to all the pairs that can be formed by combining the samples

across the sampling sites for a given sampling time, and by combining the samples taken at different times at a given sampling site. The KS test is based on the following two-sided test statistic (Conover, 1999):

$$T = \sup_x |F_i(x) - F_j(x)| \quad (5)$$

where F_i is the cumulative density function (CDF) of the i -th sample and $\sup|\cdot|$ is the sum of the differences between the two sample CDFs. The p value of the H_0 hypothesis that the two samples belonged to the same population was computed using the Python function *stats.ks_2samp* of the Python package *scipy* (Virtanen et al., 2020).

Finally, trait community-weighted means (TCWM) were calculated to quantify the proportion or weight of each trait modality in each sampled community (Table S3). TCWM is a good indicator of the expected functional value of one trait in a random community sample (Pla et al., 2012).

2.5.4. Functional indices

Functional diversity (FD) between communities was quantified using the following five multi-trait functional indices (Villéger et al., 2008; Laliberté and Legendre, 2010; Pla et al., 2012): functional richness, divergence, evenness, and dispersion, and Rao's quadratic entropy. Functional richness (FRic) is the amount of functional space occupied by the community (Villéger et al., 2008), and functional evenness (FEve) measures the distribution of abundance within the functional trait space (Villéger et al., 2008). Conversely, FDiv quantifies how the trait values are spread along the range of a trait space (Villéger et al., 2008), and functional dispersion (FDis) is the mean distance in the multidimensional trait space of individual species to the centroid of all species and estimates the dispersion of species in the trait space (Laliberté and Legendre, 2010).

Rao's quadratic entropy (RaoQ) is conceptually similar to FDis and may be seen as the expected value of the conflict among species (Ricotta and Szeidl, 2006); it includes both species relative abundances and a measure of the pairwise distances between species (Rao, 1982; Botta-Dukát, 2005). The TCWM matrix and functional indexes were computed by running the function *dbFD*, which is included in the *FD* package, implemented in the R software (Laliberté and Legendre, 2010).

The functional structure of invertebrate communities and changes in functional trait composition in space and time were assessed using a fuzzy correspondence analysis (FCA) on the TCWM. The FCA was performed with the R package *ade4* (Chevenet et al., 1994).

We used multivariate ordination (redundancy analysis (RDA)) to explore relationships among the 29 biological trait states and 73 taxa, following Poff et al. (2006). Accordingly, we ran the *rda* function included in the R package *vegan* on the $\log(x+1)$ transformed taxon abundance (Legendre and Legendre, 2012; Oksanen et al., 2013). For the rendering graph, taxa were represented using 15 different attributes to separate the genera *Diamesa*, other Diamesinae, Orthocladiinae, Chironominae, Tanyptodinae, other Diptera, Ephemeroptera, Plecoptera, Trichoptera, Coleoptera, and non-insects (Hydracarina, Crustacea, Oligochaeta, Nematoda, Tricladida) (Figure 8A). In Figure 8C, we reduced the number of groups to six, considering the order level for insects and grouping together all non-insects. Dominant trait contributions were represented, where the length of the vector was related to the strength of its contribution to the principal axes (Figure 8C).

The relationships between environmental variables (distance from the source, glacial index, and mean maximum water temperature) and indices were tested using Pearson's correlation. Statistical significance was set at $p < 0.05$. These analyses were performed using the STATISTICA version 12.0 computer package (© Statsoft).

3. Results

3.1. Air and water temperature

Figure 2 shows the monthly mean of the interpolated maximum air temperature (Tamax, dashed lines) the monthly mean of the modelled maximum water temperature (Twmax, solid lines). The time series were organized in groups representing 5 successive years, with the line representing the average, and the shaded area representing the envelope of the five monthly values. The average values taken over five years demonstrated changes in the air and river water temperatures that affected the area since the beginning of the 90's.

In winter, from December (month 12) to March (month 3), air temperature first decreased progressively in the four periods between 1990 and 2009 and then increased, attaining, in the interval $2015 \div 2020$, a similar value of the period $1990 \div 1995$. In the last 30 years, the maximum winter air temperature has increased by approximately 2.5°C . In the decade $1990 \div 1999$, the air temperature did not change appreciably in the month of April; however, it increased rapidly to approximately 3.5°C in 2020 compared to that in $1990 \div 1994$. September mirrored April, but with a marginal increase. From May to July, the pattern was similar, but with an even sharper rise of about 2.5°C starting from 2015. We observed a different pattern in August, with an initial cooling of approximately -3°C from 1990 to 2009, followed by a gradual warming that attained a global increase of approximately 1.6°C in the period $1995 \div 2020$. Finally, no significant changes in the air temperature were observed in October and November. Overall, Figures 2a-d show a complex temporal pattern of air temperature with progressively warmer springs and falls, resulting in a warm season that became progressively longer. This

overall tendency was observed at all sampling sites from CR2 to CR0.

As expected, the water temperature was the lowest at CR0, which was at the highest elevation among the four sampling stations, and it increased moderately in the last 30 years (Figure 2a). The highest water temperature was observed at CR1bis (Figure 2c), for which we took samples from a non-glacial spring, while a progressive increase in the water temperature was observed when moving from CR0 to CR1 (Figure 2b) and CR2 (Figure 2d), as an effect of the higher air temperature, longer exposure to solar radiation, and CR2, mixing with non-glacial water coming from the spring sampled at CR1bis.

In 2004, the monthly mean of the maximum daily water temperature started to rise at all the sampling locations, with a similar maximum increase of approximately 5°C in August for CR1, CR1bis, and CR2 (the mean value across the three sites was $4.73^{\circ}\text{C} \pm 0.54^{\circ}\text{C}$) and a maximum increase of 2.10°C in September for CR0. At first glance, it may be puzzling that the water temperature rose more than the air temperature in the last 10 years at CR1, CR1bis, and CR2. The reason for this behaviour was the reduction in water discharge (see Figure 3) and the corresponding reduction in the water depth and stream velocity. The overall effect of these changes was a reduction in the streamflow volume and an increase in the transit time from CR0 to CR2. Consequently, the smaller water volume absorbed more energy because of the longer exposition, and led to a larger rise in temperature. This is indirectly confirmed by the small increase observed at the sampling station CR0, which was close to the mouth of the glacier, where the increase in water temperature was smaller than that of the air and of the other sampling sites.

Inspection of Figure 2a-d, supplemented by the analysis of the data, revealed that the increase in water temperature was delayed when compared to that of the air temperature. A clear pattern of increasing water temperature emerged around the year 2000 for CR1 and CR2 and 2005

for CR0, which was approximately 20 years after we began to observe the increasing pattern in air temperature.

A synthesis of the changes in the meteorological and hydrological variables is presented in Figure 3, where the summer average (from June to September) of maximum daily temperatures (air and water) and runoff were compared in the 50 years from the 1970's to 2020. In addition, the 5-years moving averages of air temperature (dark grey dashed line) and summer water runoff (green thick solid line) are also shown. The reduction in glacial area over time (unpublished data of the last author) is also shown in the figure, together with the number of taxa and the functional richness in the years 2001, 2014, and 2018, when the sampling was performed. The yearly mean of the daily maximum air temperature showed significant oscillations, which tended to mask long-term variations. However, the 5-years average showed a clear increasing pattern. Water and air temperatures have been observed to increase since the beginning of this century and, in the same period, the summer water yield and glacier surface declined dramatically.

The first tipping point in the dynamics of the glacier area occurred in 1981, when the area started to decline at a rate of $-7ha\ y^{-1}$, until 1995. In the same period, the daily maximum air temperature increased by $1.27^{\circ}C$ (the 5 years moving averaged increased by $1.07^{\circ}C$) and the runoff also increased, reaching a peak of approximately $2700mm$ in 1995 ($39mm\ y^{-1}$). Beginning from 1995, the runoff first declined slightly to about $2400mm$ in 2003, and then more dramatically to about $400mm$ in 2019. From 2003 onwards, the water temperature increased as a combined effect of the rise in air temperature and the changed hydrodynamic conditions due to the reduced runoff discussed earlier. In the last decade, air and water temperatures experienced the strongest rise of the entire study period, while the runoff decreased sharply, and the glacier area reduced at a lower rate.

3.2. Changes in the invertebrate community structure and biomass

Across the four sites, 73 taxa were identified, with a total of 10,972 individuals. With 38 taxa, chironomids (Diptera Chironomidae) accounted for 67% of the collected fauna, and overall *Diamesa* (Diamesinae subfamily) was observed in all sampling units, with 29% of the total abundance for all sampling units combined. Four taxa were collected in only one sampling unit (Dixidae, *Brachyptera* sp., Hydraenidae, and Ostracoda), all exclusive to the spring-fed stream (CR1bis). Alpha diversity (number of taxa and Shannon index) increased with decreasing glacial influence, that is, with increasing distance from the glacier snout ($r = 0.61$; $p < 0.0001$) and decreasing ice-melt input as GI (reported in Table S1) ($r = -0.67$; $p < 0.0001$), and increasing mean maximum water temperature (reported in Table S1) ($r = -0.67$; $p < 0.0001$) (Table 3). Beta diversity ranged from 0.29 (between CR1bis sampled in 2001 and CR1bis sampled in 2018) to 1.00 (between CR0 and CR1bis) (Table 3). Alpha diversity increased through time at all sites with the number of taxa and Shannon diversity, except in CR1.

The highest beta diversity (> 0.90) was observed between kryal (CR0 and CR1) and the glacio-rhithral (CR2) and krenal (CR1bis) types, independent of the sampling year. The taxa that contributed the most to community distinctions between habitat types (SIMPER, Table S4) were mainly the Diamesinae and Orthocladiinae species followed by EPT (Ephemeroptera, Plecoptera, and Trichoptera). Specifically, *D. steinboeckii* characterised the kryal region, partly replaced over time by *D. zernyi*, which was previously observed abundantly in the glacio-rhithral and krenal regions. Other *Diamesa* species were absent in the kryal region (mainly in the metakryal CR0), for example, *D. bertrami* and *D. cinerella* gr. *D. goetghebueri*, and *Protonemoura* sp. and Empididae distinguished the glacio-rhithral (CR2) region from the others. *Pseudodiamesa branickii* and most

of Orthocladiinae were identified in the krenal region (CR1bis) every year, besides other Diptera (*Prosimulium* spp., *Simulium* spp.), Ephemeroptera (*Baetis alpinus* and *Rhitrogena loyolea*), Plecoptera (*Leuctra* spp. and *Perlodes intricatus*, Oligochaeta, Nematoda, Copepoda, Harpacticoida, and Triclada.

The biomass ranged from 0.1 mg (non-insects) to 101 mg (Coleoptera Dytiscidae) (Table S2). The violin plot (Figure 4) was highlighted as in 2001 (CR1) and in 2014 (CR0), the two uppermost sites, hosted species relatively small, to which heavier species were added in 2018. This distribution was mainly due to the increasing number of *D. zerrugi* at both sites, which had a higher mass (4.8 mg) than *D. steinboecki* (1.2 mg).

3.3. Functional changes in the community structure

Spatio-temporal variations have been highlighted for functional diversity (Figure 5, Table S5). The lowest value of all indices was calculated for CR0 independent of the year, attaining values in CR1 that were comparable with those of CR2 and CR1bis. FEve and FDiv did not change among sampling units; FEve ranged from 0.3 to 0.6 and FDiv between 0.7 and 0.9. FDis and RaoQ were lower in CR0 (minimum 2.1 and 7.8, respectively) than in the other sites (> 3.9 and > 18.9 , respectively). Only FRic increased significantly with increasing distance from the snout ($r = 0.63$, $p = 0.01$) and mean water temperature ($r = 0.59$, $p = 0.02$), independent of the year. For all the sites except CR1bis, FRic increased through time (Table S5). The minimum FRic was observed at CR0 in 2014 (0.5) and the maximum value at CR1bis in 2001 (167.7).

Figure 6 (polar bar chart) shows the relative trait composition of the nine sampling units displayed as community-weighted means (TCWM). For the sake of clarity, we excluded traits that did not vary in time and/or in space, as shown by the KS analyses (Figures S1, S2): TerPU, PLA,

SPIR, SHR, TEGU, FIL. The differences between trait categories were evidenced through the length of their bars. Based on their bar length, high values of DET, COLD, UNIV, CR, AqPu, and AeAd were associated with glacial sites (with weighted means of about 3 in the kryal and 2 in the glacio-rhithral). AeAd, CR, and DET bars were the longest ones even at CR1bis but with lower lengths than in the other sites.

GAFF, COLD, and UNIV were significantly (KS, $p < 0.05$) higher in kryal sites (CR0 and CR1) in all sampling years, with decreasing intra-site values. Generally, the presence and abundance of taxa with the highest glacial affinity and cold stenothermy decreased at all sites throughout the study period. Specifically, as reported above, the abundance of the taxon with the highest glacial affinity *D. steinboeckii* decreased in kryal sites in this time frame (-36% at CR0 and -69% at CR1) and disappeared in the glacio-rhithral site (CR2). In the kryal sites, other Diamesinae settled up or were found to be more abundant in time, that is *D. zernyi*, in addition to the first arrival of *P. parva*. For these species, the increasing value of the BIG trait and biomass was associated with CR0 and CR1 in 2013. Furthermore, at all sites, DIAP significantly (KS, $p < 0.05$) decreased and NoRES significantly (KS, $p < 0.05$) increased through time, in addition to MULTIV at CR2 and CR1bis (KS, $p < 0.05$). Figure 6 facilitates the interpretation of the fuzzy analysis results shown in Figure 7.

Fuzzy correspondence analysis revealed temporal and spatial effects on the functional structure of invertebrate communities (Figure 7 and 8). Specifically, sampling units were (i) spatially distributed along the first axis (explaining 62.2% of total variability) from right to left, with the kryal sites (CR0 and CR1) on the right (quadrant I and IV), krenal site (CR1bis) on the left (II and III quadrant), and the glacio-rhithral site CR2 in the middle, and (ii) temporally distributed along the second axis (explaining 25.3% of total variability) with sites sampled in 2001 in

quadrants III and IV, and those from 2014 and 2018 in I and II (with the sole exception of the glacio-rhithral site CR2 sampled in 2001 in quadrant I). Both axes were correlated with a wide range of functional traits (Figure 7 and Table S6). The first axis was positively correlated ($r > 0.5$) with DIAP, GAFF, and AqPU, and negatively correlated with NoPU, NoRES, and WARM. The second axis was positively correlated ($r > 0.5$) with AeAD, BIG, and AqPU, and negatively correlated with SMALL, AqAD, and NoPU. Therefore, traits that experienced major changes in time and/or space were associated with life history (body size, adult life stage, pupation), resistance forms (diapausal stage and no forms of resistance), temperature preference (thermophilic), and ecology (glacial affinity).

3.4. Correlations among traits across taxa

The multivariate summary of the taxa (Figure 8) showed separation in 2-dimensional space, where the 1st and 2nd RDA axes explained 68.7% and 28.9% of the variation in trait space, respectively. A discernible separation among 15 taxa groupings was highlighted in this ordination space (Figure 8A), although some of them (Orthocladiinae and other Diptera) contain taxa that spanned much of the ordination space and overlapped in their trait composition with others (Figure 8C, Table S7). The first trait gradient (positive axis I and negative axis II) primarily represents some species of the genus *Diamesa* and a few other Diptera (e.g. Simuliidae), although other taxa were included. The primary trait states showed high glacial affinity (GAFF), semivoltinism (SEMIV), cold stenothermy (COLD), diapausal stage (DIAP), holometabolic development with aquatic pupal stage, and detritivorous feeding mode (DET) (Figure 8B). The 2nd trait gradient (negative axis I scores and negative axis II scores) primarily represents some species of the genus *Diamesa*, Orthocladiinae, other Diptera, Plecoptera (mainly Nemouridae), Trichoptera

(Limnephilidae), and Coleoptera. The primary trait states were small size (SMALL) and univoltinism (UNIV) associated with *Diamesa*, other Diptera (e.g., *Cheilotrichia* sp.) and some Plecoptera (*Protonemoura* sp., shredders (SHR), respiration with spiracles (SPIR) or plastron (PLA). The 3rd trait gradient (positive axis I and negative axis II scores) contained Tanypodinae, some Orthocladiinae, some other Diptera, some Plecoptera (mainly Perlodidae), some Trichoptera (mainly Rhyacophilidae), and some Coleoptera that were characterised primarily by high thermophily (WARM), predation as the main food habit (PRE), aquatic adults (AqAD), good swimmers (SW), and absence of resistance forms (NoRES). Finally, the 4th trait gradient (positive axis I and positive axis II) represented mainly other Diamesinae, some Orthocladiinae, few other Diptera, all Ephemeroptera, and most non-insects that were characterised primarily by multivoltinism (MULTIV), scraper feeding habit (SCFA), resistant eggs (EGGS), and respiration by tegument (TEGU).

4. Discussion

This study provided new insights into the response of stream invertebrate communities to global warming in alpine glacial streams. In the study area, located in the Southern European Alps, the climate became warmer from the 1980s to the last decade, with a mean maximum daily summer air temperature (mT_{max}) increasing by 1.7°C at 2642 m a.s.l. and 1.8°C at 2858 m a.s.l. This is in line with recent large-scale studies extended to the entire European Alps (see for example Beniston et al., 2018).

In the last decade, the annual average of the daily maximum air temperature increased by $1.2\text{--}1.5^{\circ}\text{C}$ with respect to the previous decade in the altitude range of the sites studied (2642–2858 m a.s.l.). This increase was faster than the global average ($+0.2\pm 0.1^{\circ}\text{C}$ per decade,

(Trenberth et al., 2007; IPCC, 2018). These findings confirm that the European Alps are experiencing greater warming compared to other regions and the global average (for example, Gobiet et al., 2014; Hock et al., 2019; Niedrist and Füreder, 2021). At the elevation of CR2 (2642 m a.s.l.), which is close to the Careser dam meteorological station, we observed an annual mean warming rate of approximately 0.5°C per decade beginning from 1980, confirming a previous study by Gobiet et al. (2014).

In addition to the observed warming of air temperature, this study shows that the stream water warmed significantly since 2003, 20–25 years after the rise of air temperature and at a rate of $0.22^{\circ}\text{C y}^{-1}$ between 2003 and 2020, similar to what was observed in the last decade in several streams, such as in northern Germany (Arora et al., 2016). In 2020, the annual mean of the maximum daily water temperature reached 8.1°C at 2642 m a.s.l. and 2.4°C at 2858 m a.s.l., with increments of 4.4 and 1.6°C , respectively, with respect to the pre-2003 averages. These findings were in line with those observed in a number of Italian and Swiss rivers at an altitude of approximately 300 m a.s.l. (Lepori et al., 2015), in the period 1976–2012. The latter reported warming rates between $0.04^{\circ}\text{C y}^{-1}$ and $0.12^{\circ}\text{C y}^{-1}$, which compared well with the value of $0.04^{\circ}\text{C y}^{-1}$ obtained at CR2 (2642 m a.s.l.). Furthermore, we observed a summer warming rate of the glacier-fed stream at 2.3 km and 1.2 km downstream from the glacier ($+0.27^{\circ}\text{C y}^{-1}$ and $+0.19^{\circ}\text{C y}^{-1}$ respectively), between 2010 and 2017, comparable with that reported by Niedrist and Füreder (2021) for mountain streams in the Austrian Alps for the same period (i.e. $+0.25^{\circ}\text{C y}^{-1}$). In the same period, the metakryal site (at 0.8 km downstream from the glacier snout) and the krenal site warmed at a lower rate ($+0.10^{\circ}\text{C y}^{-1}$ and $+0.12^{\circ}\text{C y}^{-1}$ respectively), differently from what observed for non-glacial streams by Niedrist and Füreder (2021), probably due to the lower

altitudinal range of the Austrian non-glacial streams included in their work (< 2200 m a.s.l.). The warming rates of the sites evaluated in this study changed slightly if we consider the period 2003÷2020, ranging from $0.08^{\circ}\text{C y}^{-1}$ for CR1bis to $+0.22^{\circ}\text{C y}^{-1}$ for CR2.

Concurrently, since 1980, the Careser glacier exhibited gradual surface area reduction, with a decreasing rate of -9.3ha y^{-1} in the period 1980–2011 and -5.3ha y^{-1} from 2011 to date. With such rates, the glacier lost 3.5km^2 of the surface since 1980 ($= -74\%$). The loss rate of the glacial area was in line with the observations of Zemp et al. (2015), who reported a loss of 53% for central Europe during the period 2001÷2010, comparable with the current observations of 40%. As a consequence of this warming dynamics, in the first phase, the glacier runoff increased (up to 1995), following which it decreased gradually, reaching a rate of -130mm y^{-1} in the last decade. In the last 20 years, the loss rate of runoff was $3.7\% \text{ y}^{-1}$ (compared to 1999), which is an overestimation when compared to the value of $0.6\% \text{ y}^{-1}$ reported in Michel et al. (2020), between 1999 and 2018, for nine streams in Switzerland (between 1951 and 2624 m a.s.l.). It is evident that the Careser stream had already crossed the hydrological tipping point of the maximum summer discharge associated with glacier disappearance (Huss and Hock, 2018).

Invertebrate sampling in 2001 provided a snapshot of the community before 2003, that is, before the onset of stream water warming. Thirteen to seventeen years after the first sampling, both taxa richness and Shannon diversity increased in CR2, CR1, and CR1bis. This was evident also in CR0 sampled in 2018 after only 4 years from the first campaign in this site, concurrently, in CR0, to an increase in mean summer water temperature from 1.7 to 2.2°C . The increase in functional diversity was more evident in the metakryal CR0, where FRic changed from 0.48 to 6.74 in only 4 years, and in the hypokryal CR1, where FRic changed from 42.64 to 69.50 in 17 years. The arrival

of new species, even with few individuals, brought new traits in the community (e.g. with the colonisation of metakryal CR0, where the maximum water temperature did not change considerably, remaining approximately 2°C) by other Diamesinae than *Diamesa* species *P. parva* and Orthocladiinae (e.g. *Parorthocladius nudipennis*). More Orthocladiinae and other Diptera (*Cheilotrichia* sp.) conquered CR1, where in 2018 the maximum water temperature reached the limit value of approximately 6°C . This was coupled with a decrease in *Diamesa steinboecki* abundance, as expected (Füreder and Niedrist, 2020; Lencioni et al., 2021). Functional increase was less sharp in the glacio-rhithral site CR2 (evident only after 17 years from the first sampling) and was absent in the krenal. At CR2, a complete invertebrate community was still occurring the site in 2001, and the results suggested that the upstream or inter-stream migration regarded first taxa with similar traits as the local species (functional redundancy), responding to a gradual change in environmental conditions. Here, the spread of taxa with functional strategies different from those previously characterising the site (e.g. increase of multivoltine taxa with large body size, no resistance forms, and water tolerance), combined with the tolerance of some resident species to present-day conditions (mainly within Diamesinae), has resulted in an increase in FRic. Hence, the lag in the fauna response in terms of functional diversity to the climatic conditions of the CR2 site appeared to be approximately 17 years. When the discharge dropped below 700 mm ($< 0.5\text{ m}^3\text{ s}^{-1}$), the mean maximum water temperature remained above 7.5°C , and mean maximum air temperature above 12°C . The main change that occurred in CR2 was the decline in abundance (in 2014) and consequent disappearance (in 2018) of *Diamesa steinboecki*. This was the species with the highest glacial affinity, recognised as a "flag" species and an indicator of the transition from kryal to glacio-rhithral type (Lencioni et al., 2021). Its disappearance can be explained by the warming of this stream sector from 3.4°C in 2001 to 6.1°C in 2014 and 8°C in 2018,

exceeding the upper thermal survival of this species = 6°C , Lencioni (2018). This thermal value was reported by Niedrist and Füreder (2021) as the upper value of the optimal thermal range for several Diamesinae occurring in glacial habitats. As expected (Milner et al., 2001; Brown et al., 2018), minor changes occurred in the krenal community at CR1bis in 17 years owing to unchanged hydrological conditions (Lencioni, 2018), and were not directly affected by glacier retreating. This was observed notwithstanding the increase in the maximum water temperature in CR1bis, from 8.4°C in 2001 to 10.6°C in 2018. This increase was consistent with the literature highlighting the warming even of groundwater and springs at high altitudes under climate change (Menberg et al., 2014; Kürty et al., 2017). However, the water temperature remained in the range favourable to the species occurring the site in 2001, justifying the minor changes observed. Additionally, in this stream type, a wider distribution of body mass was observed, suggesting the occurrence of all body mass values, from lighter (e.g. non-insects) to heavier species (Plecoptera Perlodidae, Trichoptera, Rhyacophilidae, and Coleoptera).

Predictably, a process of gradual taxonomical homogenisation was evident from the beta diversity (e.g. beta diversity decreased between CR1 and CR2 from 2001 = 0.89 to 2018 = 0.82) (Cauvy-Fraunié et al., 2016), which was further confirmed by the decreasing beta diversity between krenal and the other two stream types from 2001 to 2018.

All FD indices, apart from FDiv, were found to be lower in sites with higher GI and GCC, as observed by Brown et al. (2018). However, only FRic increased significantly in space and time with less glacial influence, reflecting a greater diversity of traits. Therefore, we suggest that this might be the best predictor of changes in functional diversity under glacier retreat. FEve showed more regular distributions of organisms in the trait space with decreasing glacial influence, demonstrating greater niche saturation, implying that resistance to new colonisers becomes

stronger in more benign habitats (Harrison and Cornell, 2008). FDis and RaoQ also increased significantly with declining glacial influence (after separating CR0 from the other sites). This indicated that dominant species were located further from the centre in trait space, suggesting greater competition and/or the opening up of new, distinct niches in more favourable (less extreme) habitats.

Correlations among traits across Taxa (RDA), highlighted as specific sets of trait states, resulted in strong associations with particular groups of taxa, a finding similar to that reported for the European lotic insect taxa using different traits (Usseglio-Polatera et al., 2000). We highlighted the high heterogeneity of traits within the chironomids, with a clear distinction between the *Diamesa* genus and Tanypodinae. Orthocladiinae exhibited traits that overlapped with many other non-chironomid taxa. Similarities in trait analyses were also observed within Coleoptera, Ephemeroptera, and non-insects, whereas Hymenoptera, Trichoptera, and other Diptera accounted for high trait heterogeneity at the order level (the highest one for Diptera as a whole, as expected in Courtney et al. (2017)), because they possess diverse trait characteristics among the constituent genera and species. Thus, to capture the amount of variation in trait diversity within benthic communities, a coarse taxonomic resolution is not recommended; Diptera and EPT are the main colonisers of such habitats (Lencioni, 2018). This grouping suggested that the trait composition of the communities changed (i) with decreasing distance from the glacier-snout and the ice-melt inputs, independently of the year of sampling; (ii) through time at each site, as highlighted by FCA. Overall, FCA detected a spatio-temporal shift in some functional traits related mainly to life cycle, physiology, resistance, diet, and ecology as a response to reduced glacial influence. Trait shifts were associated mainly with the reduction and subsequent disappearance of the stenothermal species that were adapted to the cold (*Diamesa steinboecki*) in all glacial sites. Additionally, cold

stenothermal taxa were partially replaced by eurythermal warming-tolerant taxa, even larger, multivoltine and with a more variegated diet (e.g. Orthocladinae and EPT), mainly in the glacio-rhithral site. FCA confirmed an increasing similarity between the glacio-rhithral and krenal sites, emphasising the role of recruitment of new taxa of the non-glacial tributary. Some taxa (and related traits) have not yet migrated from the tributary to the glacio-rhithral region, which continues to be an inhospitable environment for taxa (e.g. due to too high current velocity) such as Ostracoda, Crustacea, and Coleoptera.

5. Conclusions

Understanding the vulnerability of alpine glacier-fed ecosystems to climate change and their consequences is challenging. This work provides new insights into how late glacier-fed and non-glacial ecosystems respond to global warming, with respect to water temperature and community structure and function. There are specific functional traits present in the taxa that are most associated with high glaciality (some *Diamesa* species); these traits enable them to live in harsh environmental conditions and will be lost in kryal regions with the loss of these species. These results might be useful for predicting responses to climate change for other systems for which long-term data sets on runoff, glacier surface, and air and water temperature are not available. Specifically, they offer the potential for predicting the timing of change both in the amount of water available for different uses. Moreover, it could predict the timing and mode of change in animal community structure and function, thereby affecting the ecosystem services dependent on them. Finally, to monitor faunal changes, we recommend sampling invertebrate communities in such habitats at a frequency of approximately ten years for systems fed by glaciers larger than 3 km^2 , and at a frequency of three or five years for smaller glaciers, to intercept the

shifts in community structure and function without increasing the risk of extinction of kryal species due to oversampling (Lencioni and Gobbi, 2021).

Acknowledgements

The authors thank Matthew Becker (California State University, Long Beach) for his collaboration in collecting water temperature data in 2010; Alessandra Franceschini, Daniele Debiasi, and Francesca Paoli (MUSE) who participated in biological sampling, and Efisio Siddi and Gianluca Tognoni (Meteotrentino) for managing the gauge station at CR2 and Alberto Trenti for coordinating Meteotrentino activities. The authors thank Roberto Seppi (University of Pavia, Italy) for providing the pictures of the Careser glacier used in the Graphical Abstract, shot in 1970 by Giorgio Zanoni and in 2012 by Luca Carturan (University of Padua, Italy).

References

- Arora, R., Tockner, K., Venohr, M., 2016. Changing river temperatures in northern Germany: trends and drivers of change. *Hydrological Processes* 30 (17), 3084–3096.
- Beniston, M., Farinotti, L., Stoffel, M., Andreassen, L. M., Coppola, E., Eckert, N., Fantini, A., Giacomoni, F., Hauck, C., Huss, M., Huwald, H., Lehning, M., López-Moreno, J.-I., Magnusson, J., Marty, C., Morán-Tejeda, E., Morin, S., Naaim, M., Provenzale, A., Rabatel, A., Six, D., Stötter, J., Strasser, U., Terzago, S., Vincent, C., 2018. The European mountain cryosphere: a review of its current state, trends, and future challenges. *The Cryosphere* 12 (2), 759–794.
- Botta-Dukát, Z., 2005. Rao's quadratic entropy as a measure of functional diversity based on multiple traits. *Journal of Vegetation Science* 16 (5), 533–540.
- Bray, J. R., Curtis, J. T., 1957. An Ordination of the Upland Forest Communities of Southern

- Wisconsin. *Ecological Monographs* 27 (4), 326–349.
- Brighenti, S., Tolotti, M., Bertoldi, W., Wharton, G., Bruno, M. C., 2021. Rock glaciers and paraglacial features influence stream invertebrates in a deglaciating Alpine area. *Freshwater Biology* 66 (3), 535–548.
- Brighenti, S., Tolotti, M., Bruno, M. C., Engel, M., Wharton, G., Cerasino, L., Mair, V., Bertoldi, W., 2019. After the peak water: the increasing influence of rock glaciers on alpine river systems. *Hydrological Processes* 33 (21), 2804–2823.
- Brown, L. E., Hannah, D. M., Milner, A. M., Soulsby, C., Hodson, A. J., Brewer, M. J., 2006. Water source dynamics in a glacierized alpine river basin (Taillon-Gabiétous, French Pyrénées). *Water Resources Research* 42 (8).
- Brown, L. E., Khamis, K., Wilkes, M., Blaen, P., Püttlin, J. E., Carrivick, J. L., Fell, S., Friberg, N., Füreder, L., Gislason, G. M., et al., 2015. Functional diversity and community assembly of river invertebrates show globally consistent responses to decreasing glacier cover. *Nature Ecology & Evolution* 2 (2), 325–333.
- Bruno, D., Belmar, O., Maire, A., Morel, A., Dumont, B., Datry, T., 2019. Structural and functional responses of invertebrate communities to climate change and flow regulation in alpine catchments. *Global Change Biology* 25 (5), 1612–1628.
- Caissie, D., 2006. The thermal regime of rivers: a review. *Freshwater Biology* 51 (8), 1389–1406.
- Calow, P., 1989. Proximate and ultimate responses to stress in biological systems. *Biological Journal of the Linnean Society* 37 (1-2), 173–181.
- Carturan, L., Baroni, C., Becker, M., Bellin, A., Cainelli, O., Carton, A., Casarotto, C., Dalla Fontana, G., Godio, A., Martinelli, T., Salvatore, M. C., Seppi, R., 2013. Decay of a long-term monitored glacier: Careser Glacier (Ortles-Cevedale, European Alps). *The Cryosphere* 7 (6), 1111–1121.

1819–1838.

- Casarotto, C., Bertoni, E., 2015. Estensione dei ghiacciai trentini dalla fine della piccola era glaciale a oggi: rilevamento sul terreno, digitalizzazione GIS e analisi. MUSE-Museo delle Scienze, Trento (Italy).
- Castella, E., Adalsteinsson, H., Brittain, J. E., Gislason, G. M., Lehmann, A., Lencioni, V., Lods-Crozet, B., Maiolini, B., Milner, A. M., Olafsson, J. S., Saltveit, S. J., Snook, D. L., 2001. Macrobenthic invertebrate richness and composition along a latitudinal gradient of european glacier-fed streams. *Freshwater Biology* 46 (12), 1811–1831.
- Cauvy-Fraunié, S., Andino, P., Espinosa, R., Calvez, K., Jacobsen, D., Dangles, O., 2016. Ecological responses to experimental glacier-runoff reduction in alpine rivers. *Nature Communications* 7 (1), 1–7.
- Chen, J., Ohmura, A., 1990. Estimation of Alpine glacier water resources and their change since the 1870s. *IAHS publ* 193, 127–135.
- Chevenet, F., Dolédec, S., Chessel, D., 1994. A fuzzy coding approach for the analysis of long-term ecological data. *Freshwater Biology* 31 (3), 295–309.
- Chollet, F., 2018. Deep Learning with Python. Manning Shelter Island.
- Clarke, K. R., 1993. Non-parametric multivariate analyses of changes in community structure. *Australian Journal of Ecology* 18 (1), 117–143.
- Conover, W. J., 1999. Practical Nonparametric Statistics. John Wiley & Sons, wiley Series in Probability and Statistics: Applied Probability and Statistics Section.
- Courtney, G., Pape, T., Skevington, J., Sinclair, B., 07 2017. Biodiversity of Diptera: Science and Society. Ch. 9, pp. 229–278.
- Debiasi, D., Franceschini, A., Paoli, F., Lencioni, V., 2022. How do macroinvertebrate

- communities respond to declining glacial influence in the Southern Alps? *Limnetica* 41 (1), 121–137.
- Dickson, N. E., Carrivick, J. L., Brown, L. E., 2012. Flow regulation alters alpine river thermal regimes. *Journal of Hydrology* 464-465, 505–516.
- Fell, S. C., Carrivick, J. L., Brown, L. E., 2017. The Multitrophic Effects of Climate Change and Glacier Retreat in Mountain Rivers. *BioScience* 67 (10), 897 – 911.
- Füreder, L., Niedrist, G. H., 2020. Glacial Stream Ecology: Structural and Functional Assets. *Water* 12 (2).
- Glorot, X., Bordes, A., Bengio, Y., 2011. Deep sparse rectifier neural networks. In: *Proceedings of the fourteenth international conference on artificial intelligence and statistics. JMLR Workshop and Conference Proceedings*, pp. 315–323.
- Gobbi, M., Ambrosini, R., Casarotto, C., D'Alaiuti, G., Ficetola, G., Lencioni, V., Seppi, R., Smiraglia, C., Tampucci, D., Valle, P., et al., 2021. Vanishing permanent glaciers: climate change is threatening a European Union habitat (Code 8340) and its poorly known biodiversity. *Biodiversity and Conservation* 30 (7), 2267–2276.
- Gobbi, M., Lencioni, V., 2020. Glacial Biodiversity: Lessons from ground-dwelling and aquatic insects. *Glaciers and the polar environment*, 143.
- Gobiet, A., Kotlarski, S., Beniston, M., Heinrich, G., Rajczak, J., Stoffel, M., 2014. 21st century climate change in the European Alps—A review. *Science of the Total Environment* 493, 1138–1151.
- Goodfellow, I., Bengio, Y., Courville, A., 2016. *Deep Learning*. MIT Press, <http://www.deeplearningbook.org>.
- Goovaerts, P., 1997. *Geostatistics for natural resources evaluation*.

- Harrison, S., Cornell, H., 2008. Toward a better understanding of the regional causes of local community richness. *Ecology letters* 11 (9), 969–979.
- Hock, R., Rasul, G., Adler, C., Cáceres, B., Gruber, S., Hirabayashi, Y., Jackson, M., Kääb, A., Kang, S., Kutuzov, S., et al., Sep. 2019. High mountain areas. Intergovernmental Panel on Climate Change, Switzerland, Ch. 2, pp. 2–1 – 2–90, https://report.ipcc.ch/srocc/pdf/SROCC_FinalDraft_FullReport.pdf.
- Hotaling, S., Finn, D. S., Joseph Giersch, J., Weisrock, D. W., Jacobsen, D., 2017. Climate change and alpine stream biology: progress, challenges, and opportunities for the future. *Biological Reviews* 92 (4), 2024–2045.
- Huss, M., Fischer, M., 2016. Sensitivity of Very Small Glaciers in the Swiss Alps to Future Climate Change. *Frontiers in Earth Science* 4, 34.
- Huss, M., Hock, R., 2018. Global-scale hydrological response to future glacier mass loss. *Nature Climate Change* 8 (2), 135–140.
- Ilg, C., Castella, E., 2006. Patterns of macroinvertebrate traits along three glacial stream continuums. *Freshwater Biology* 51 (5), 840–853.
- Immerzeel, W. W., Lutz, A., Andrade, M., Bahl, A., Biemans, H., Bolch, T., Hyde, S., Brumby, S., Davies, B., Elmore, A., et al., 2020. Importance and vulnerability of the world's water towers. *Nature* 577 (7790), 364–369.
- IPCC, 2018. Summary for Policymakers. In: *Global Warming of 1.5 °C . An IPCC Special Report on the impacts of global warming of 1.5 °C above pre-industrial levels and related global greenhouse gas emission pathways, in the context of strengthening the global response to the threat of climate change, sustainable development, and efforts to eradicate poverty.* [Masson-Delmotte, V., P. Zhai, H.-O. Pörtner, D. Roberts, J. Skea, P.R. Shukla, A. Pirani, W.

- Moufouma-Okia, C. Pan, R. Pidcock, S. Connors, J.B.R. Matthews, Y. Chen, X. Zhou, M.I. Gomis, E. Lonnoy, T. Maycock, M. Tignor, and T. Waterfield (eds.)). World Meteorological Organization.
- Jacobsen, D., Dangles, O., 2012. Environmental harshness and global richness patterns in glacier-fed streams. *Global Ecology and Biogeography* 21 (6), 647–656.
- Kaser, G., Großhauser, M., Marzeion, B., 2010. Contribution potential of glaciers to water availability in different climate regimes. *Proceedings of the National Academy of Sciences* 107 (47), 20223–20227.
- Küry, D., Lubini, V., Stucki, P., 2017. Temperature patterns and factors governing thermal response in high elevation springs of the Swiss Central Alps. *Hydrobiologia* 793 (1), 185–197.
- Laliberté, E., Legendre, P., 2010. A distance-based framework for measuring functional diversity from multiple traits. *Ecology* 91 (1), 29–39.
- Legendre, P., Legendre, L., 2012. Numerical ecology. In: Legendre, P., Legendre, L. (Eds.), *Numerical Ecology*. Vol. 24 of *Developments in Environmental Modelling*. Elsevier, p. iv.
- Lencioni, V., 2000. Chironomid (Diptera: Chironomidae) assemblages in three Alpine glacial systems. Ph.D. thesis, Leopold-Franzens-Universität Innsbruck - Austria.
- Lencioni, V., 2018. Glacial influence and stream macroinvertebrate biodiversity under climate change: Lessons from the Southern Alps. *Science of The Total Environment* 622-623, 563–575.
- Lencioni, V., Franceschini, A., Paoli, F., Debiasi, D., 2021. Structural and functional changes in the macroinvertebrate community in Alpine stream networks fed by shrinking glaciers. *Fundamental and Applied Limnology* 194 (3), 237–258.
- Lencioni, V., Gobbi, M., 2021. Monitoring and conservation of cryophilous biodiversity: concerns when working with insect populations in vanishing glacial habitats. *Insect Conservation and*

Diversity 14 (6), 723–729.

Lencioni, V., Jousson, O., Guella, G., Bernabò, P., 2015. Cold adaptive potential of chironomids overwintering in a glacial stream. *Physiological Entomology* 40 (1), 43–53.

Lepori, F., Pozzoni, M., Pera, S., 2015. What drives warming trends in streams? A case study from the Alpine foothills. *River Research and Applications* 31 (6), 663–675.

Mason, N. W., de Bello, F., Mouillot, D., Pavoine, S., Dray, S., 2013. A guide for using functional diversity indices to reveal changes in assembly processes along ecological gradients. *Journal of Vegetation Science* 24 (5), 794–806.

Matiu, M., Crespi, A., Bertoldi, G., Carmagnola, C. M., Marty, C., Morin, S., Schöner, W., Berro, D. C., Chiogna, G., Gregorio, L. D., Kotlarski, S., Majone, B., Resch, G., Terzago, S., Valt, M., Beozzo, W., Cianfarra, P., Gouttevin, I., Mercolini, G., et al., 2021. Observed snow depth trends in the European Alps: 1971 to 2019. In: *EGU General Assembly 2021*. Vol. 15. Copernicus GmbH, pp. 1343–1382, online, 19–30 Apr 2021, EGU21-3287.

Menberg, K., Blum, P., Kurylyk, R., Bayer, P., 2014. Observed groundwater temperature response to recent climate change. *Hydrology and Earth System Sciences* 18 (11), 4453–4466.

Michel, A., Brauchli, T., Lehning, M., Schaefli, B., Huwald, H., 2020. Stream temperature and discharge evolution in Switzerland over the last 50 years: annual and seasonal behaviour. *Hydrology and Earth System Sciences* 24 (1), 115–142.

Milner, A. M., Brittain, J. E., Castella, E., Petts, G. E., 2001. Trends of macroinvertebrate community structure in glacier-fed rivers in relation to environmental conditions: a synthesis. *Freshwater Biology* 46 (12), 1833–1847.

Milner, A. M., Khamis, K., Battin, T. J., Brittain, J. E., Barrand, N. E., Füreder, L., Cauvy-Fraunié, S., Gíslason, G. M., Jacobsen, D., Hannah, D. M., Hodson, A. J., Hood, E., Lencioni, V.,

- Ólafsson, J. S., Robinson, C. T., Tranter, M., Brown, L. E., 2017. Glacier shrinkage driving global changes in downstream systems. *Proceedings of the National Academy of Sciences* 114 (37), 9770–9778.
- Niedrist, G. H., Füreder, L., 2021. Real-time warming of Alpine streams: (re)defining invertebrates' temperature preferences. *River Research and Applications* 37 (2), 283–293.
- Oksanen, J., Blanchet, F. G., Kindt, R., Legendre, P., Minchin, P. R., O'hara, R., Simpson, G. L., Solymos, P., Stevens, M. H. H., Wagner, H., et al., 2013. Package 'vegan'. *Community ecology package*, version 2 (9), 1–295.
- Pedregosa, F., Varoquaux, G., Gramfort, A., Michel, V., Thirion, B., Grisel, O., Blondel, M., Prettenhofer, P., Weiss, R., Dubourg, V., Vanderplas, J., Passos, A., Cournapeau, D., Brucher, M., Perrot, M., Duchesnay, E., 2011. Scikit learn: Machine Learning in Python. *Journal of Machine Learning Research* 12, 2825–2830.
- Pla, L., Casanoves, F., Di Rienzo, J., 2012. Functional Diversity Indices. In: *Quantifying Functional Biodiversity*. Springer Netherlands, Dordrecht, pp. 27–51.
- Poff, N. L., 1997. Landscape filters and species traits: towards mechanistic understanding and prediction in stream ecology. *Journal of the north american Benthological society* 16 (2), 391–409.
- Poff, N. L., Olden, J. D., Vieira, N. K., Finn, D. S., Simmons, M. P., Kondratieff, B. C., 2006. Functional trait niches of North American lotic insects: traits-based ecological applications in light of phylogenetic relationships. *Journal of the North American Benthological Society* 25 (4), 730–755.
- Rao, C., 1982. Diversity and dissimilarity coefficients: A unified approach. *Theoretical Population Biology* 21 (1), 24–43.

- Raschka, S., 2015. Python machine learning. Packt publishing ltd.
- Ricotta, C., Szeidl, L., 2006. Towards a unifying approach to diversity measures: Bridging the gap between the shannon entropy and rao's quadratic index. *Theoretical Population Biology* 70 (3), 237–243.
- Shannon, C. E., Weaver, W., 1949. *The Mathematical Theory of Communication*. Vol. 34. University of Illinois Press.
- Smiraglia, C., Diolaiuti, G., 2015. Estensione dei ghiacciai trentini: dalla fine della piccola era glaciale a oggi: rilevamento sul terreno, digitalizzazione GIS e analisi. Ev-K2-CNR. ed., Bergamo (Italy).
- URL <http://www.glaciologia.it/catasto-dei-ghiacciai-trentini-cura-c-smiraglia-g-diolaiuti/>
- Tachet, H., Richoux, P., Bournaud, M., Usseglio Polatera, P., 2010. *Invertébrés d'eau douce: systématique, biologie, écologie*. Vol. 15. CNRS éditions Paris.
- Tlhalerwa, T., Mphale, K., 2021. Simple climate change indicators for developing countries. *Academia Letters*. *Academia Letters* (1134).
- Trenberth, K. E., Jones, P. D., Ambenje, P., Bojariu, R., Easterling, D., Klein Tank, A., Parker, D., Rahimzadeh, F., Renwick, I. A., Rusticucci, M., et al., 01 2007. *Observations: Surface and Atmospheric Climate Change*. Cambridge University Press, Ch. 3, pp. 235–336.
- Usseglio-Polatera, P., Bournaud, M., Richoux, P., Tachet, H., 2000. Biomonitoring through biological traits of benthic macroinvertebrates: how to use species trait databases? In: *Assessing the Ecological Integrity of Running Waters*. Springer, pp. 153–162.
- van Vliet, M. T. H., Ludwig, F., Zwolsman, J. J. G., Weedon, G. P., Kabat, P., 2011. Global river temperatures and sensitivity to atmospheric warming and changes in river flow. *Water Resources Research* 47 (2).

- Villéger, S., Mason, N. W. H., Mouillot, D., 2008. New multidimensional functional diversity indices for a multifaceted framework in functional ecology. *Ecology* 89 (8), 2290–2301.
- Virtanen, P., Gommers, R., Oliphant, T. E., Haberland, M., Reddy, T., Cournapeau, D., Burovski, E., Peterson, P., Weckesser, W., Bright, J., van der Walt, S. J., Brett, M., Wilson, J., Millman, K. J., Mayorov, N., Nelson, A. R. J., Jones, E., Kern, R., Larson, E., Carey, C. J., Polat, İ., Feng, Y., Moore, E. W., VanderPlas, J., Laxalde, D., Perktold, J., Cimrman, R., Henriksen, I., Quintero, E. A., Harris, C. R., Archibald, A. M., Ribeiro, A. H., Pedregosa, F., van Mulbregt, P., SciPy 1.0 Contributors, 2020. SciPy 1.0: Fundamental Algorithms for Scientific Computing in Python. *Nature Methods* 17, 261–272.
- Webb, B. W., Clack, P. D., Walling, D. E., 2003. Water–air temperature relationships in a devon river system and the role of flow. *Hydrological Processes* 17 (15), 3069–3084.
- Webb, B. W., Hannah, D. M., Moore, R. L., Frown, L. E., Nobilis, F., 2008. Recent advances in stream and river temperature research. *Hydrological Processes* 22 (7), 902–918.
- Zemp, M., Frey, H., Gärtner-Roer, I., Nussbaumer, S. U., Hoelzle, M., Paul, F., Haeberli, W., Denzinger, F., Ahlstrøm, A. P., Anderson, B., et al., 2015. Historically unprecedented global glacier decline in the early 21st century. *Journal of Glaciology* 61 (228), 745–762.

Tables and Figures

Table 1: Site description. LIA= Little Ice Age

	Mountain Group	Ortles-Cevedale
	River catchment	Noce
	Catchment area (km ²)	8.39
	Geology	Metamorphic (paragneiss, micaschists, phyllades)
	ETRS 1989 UTM zone 32N X;	631528
	Y	5144516
	Glacier area_ LIA (km ²)	6.58
Glacier	Glacier area_ 2015 (km ²)	1.39
	Retreating rate between 1987 and 2015 (% y ⁻¹)	-2.3
	Altitude glacial snout (m a.s.l.)	2976
	Altitudinal range (m a.s.l.)	2642 - 2858
	Distance from source (km)	0.75 - 2.29
Sampling sites	N. streams; N. sites	2; 4
		kryal (CR0, CR1);
	N. sites/stream type	glacio-rhithral (CR2);
		krenal (CR1bis)

Table 2: Ten biological traits (29 states or modalities) describing life history, stress resistance,

physiology, and ecology of invertebrates.

	Trait	Category	Label
Life history	Body size	Small <10 mm	SMALL
		Big >10 mm	BIG
	Voltinism	Semivoltine < 1	SEMIV
		Univoltine 1 (2)	UNIV
		Multivoltine > 2	MULTIV
	Adult life stage	Aquatic adult	AqAD
		Aerial adults	AeAD
	Pupation	Aquatic Pupa	AqPU
		Terrestrial Pupa	TerPU
		No pupation	NoPU
Stress resistance	Resistant forms	Resistant eggs	EGGS
		Diapause/dormancy	DIAP
		None resistant forms	NoRES
Physiology	Temperature preference	Cold stenothermal	COLD
		Eurythermal	WARM
	Respiration mode	Tegument	TEGU
		Gill/proth horns	GILL
		Plastron	PLA

Ecology	Living habits	Spiracle	SPIR
		Burrowers+InterstitialBU	
		Clinger-Attached	CL
	Feeding habit	Swimmers	SW
		Crawler	CR
		Detritivorous	DET
		Shredder	SHRs
		Scraper	SCRA
		Filter feeder	FILT
		Predator	PRE
	Occurrence in glacier-fed streams	Glacial affinity	GAFF

Table 3: Bray-Curtis beta diversity, number of taxa, and Shannon diversity values.

β -div	CR0_1	CR0_1	CR1_0	CR1_1	CR2_0	CR2_1	CR2_1	CR1bis_0	CR1bis_1
	4	8	1	8	1	4	8	1	8
CR0_18	0.71								
CR1_01	0.51	0.62							
CR1_18	0.80	0.43	0.63						
CR2_01	0.96	0.83	0.89	0.72					
CR2_14	0.97	0.86	0.90	0.74	0.39				
CR2_18	0.98	0.87	0.93	0.80	0.43	0.37			
CR1bis_01	1.00	0.98	0.99	0.96	0.80	0.78	0.72		
CR1bis_18	1.00	0.98	0.98	0.96	0.80	0.77	0.71	0.29	

N. taxa	4	9	14	23	47	49	59	65	67
Shannon-di	1.16	1.32	2.28	2.11	2.77	3.06	3.04	3.33	3.4

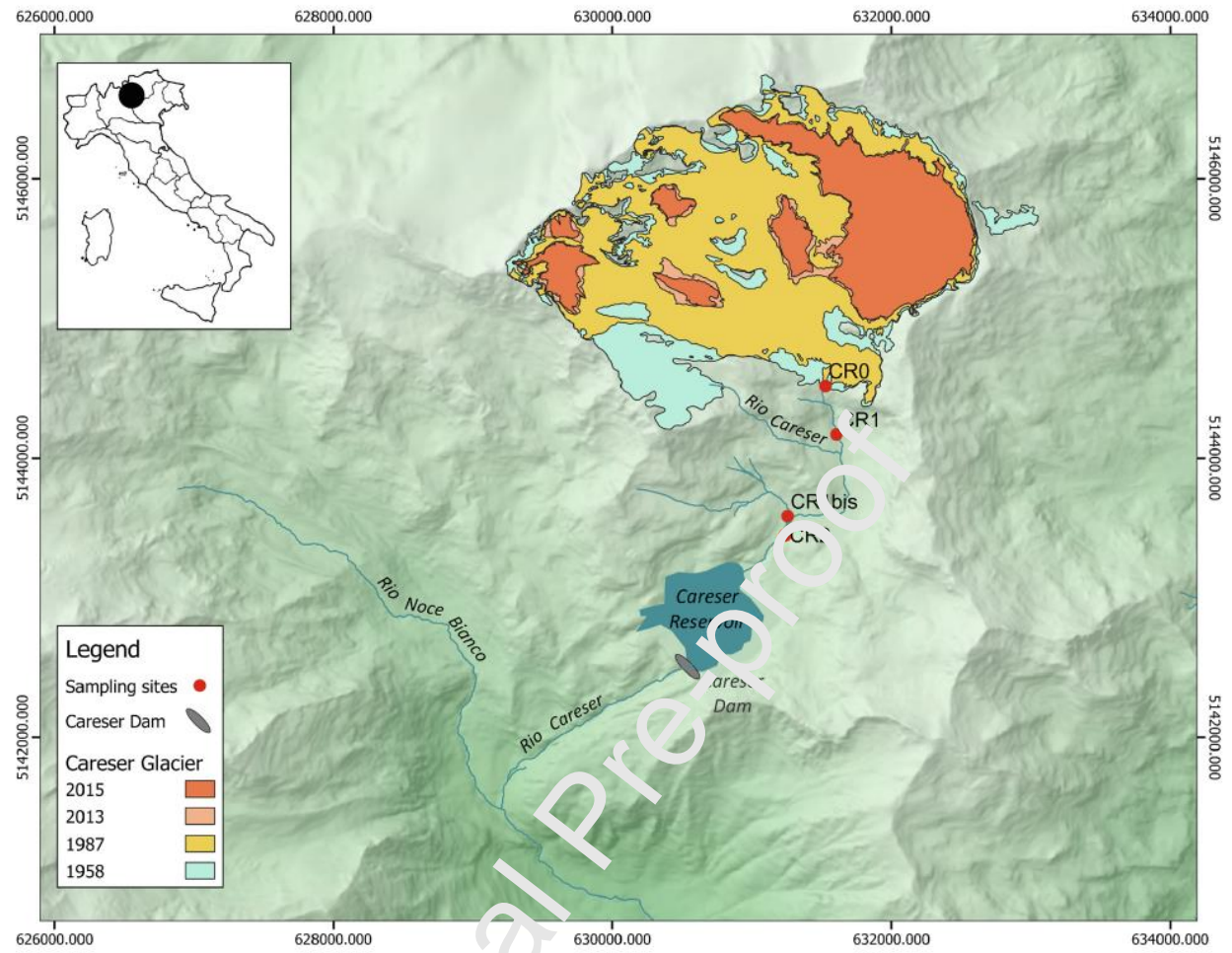


Figure 1: Map of the Careser study area. Coordinates are in the system UTM-WGS 84.

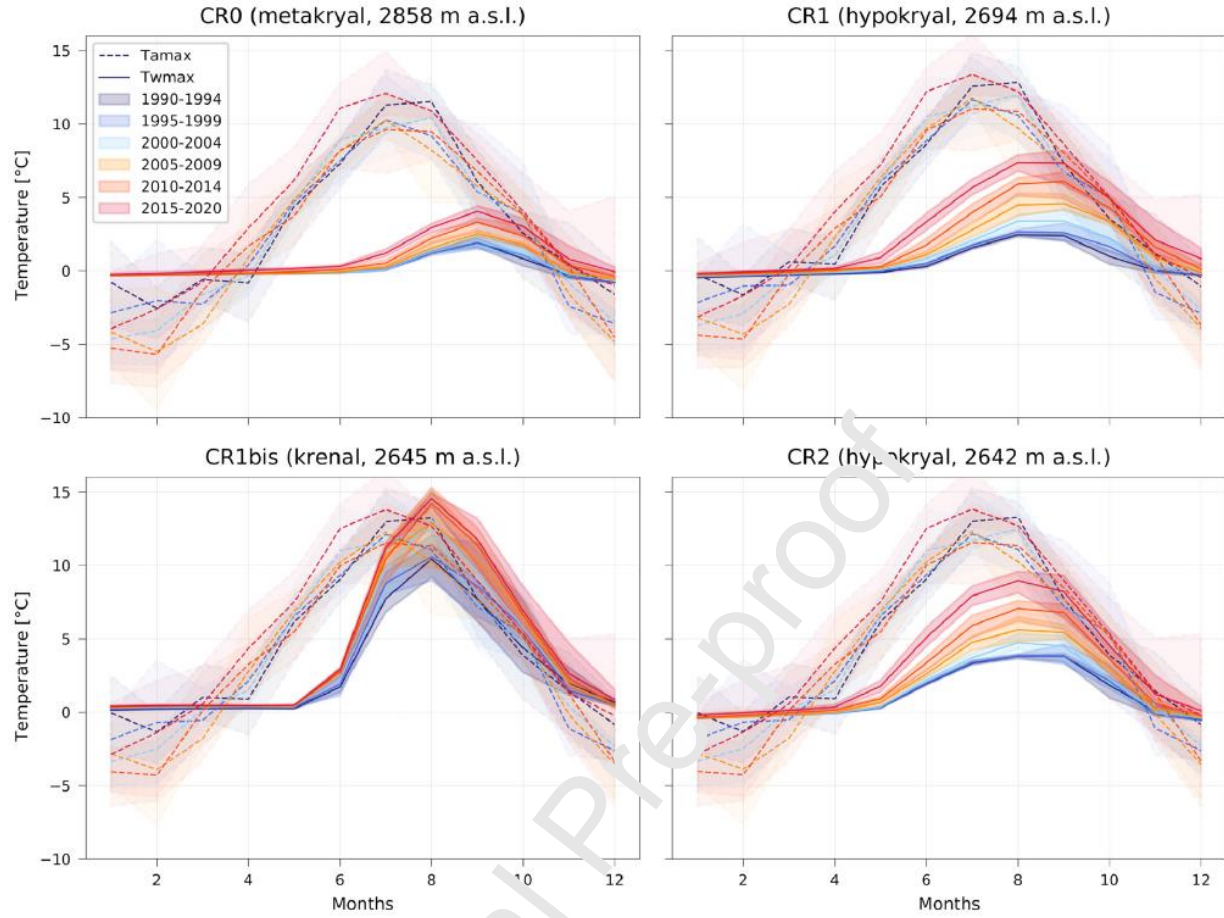


Figure 2: Maximum Air Temperature (dashed line) and Maximum Water Temperature (continued line) for investigated Stations, indicated as title of the plots. Temperatures were averaged monthly for grouped periods of five years.

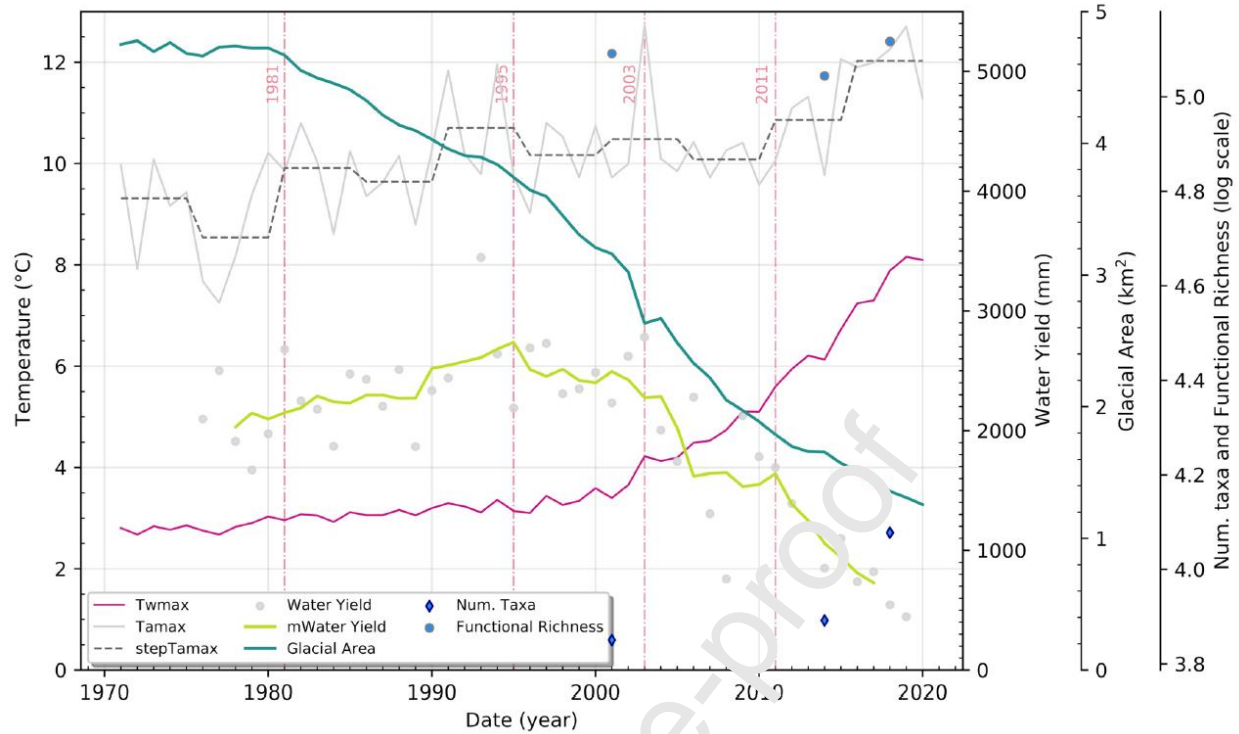


Figure 3: Comparing the most relevant climatic and biologic time series for station CR2, yearly averaged for summer period (from June to September included): daily maximum air temperature and its mean computed over blocks of 5 years ($^{\circ}\text{C}$) (solid light grey curve and dashed dark grey line); daily maximum water temperature ($^{\circ}\text{C}$) (pink line); water yield (runoff) (mm) (light grey dots) and its 5-years moving average (green line); glacier area (blue line); number of taxa (blue rhombus) and functional richness (blue dots), for three sampling years (2001, 2014, 2018). Left ordinate indicates both air and water temperatures, whereas all other quantities are reported on the right ordinates. Runoff is reported as the summer water yield (mm), that is, the total summer runoff volume divided by the contributing area at CR2. Red dashed vertical lines refer to years of main changes in air temperature (1981), water yield (1995), water temperature (2003), and of all environmental variables (2011), as explained in the text.

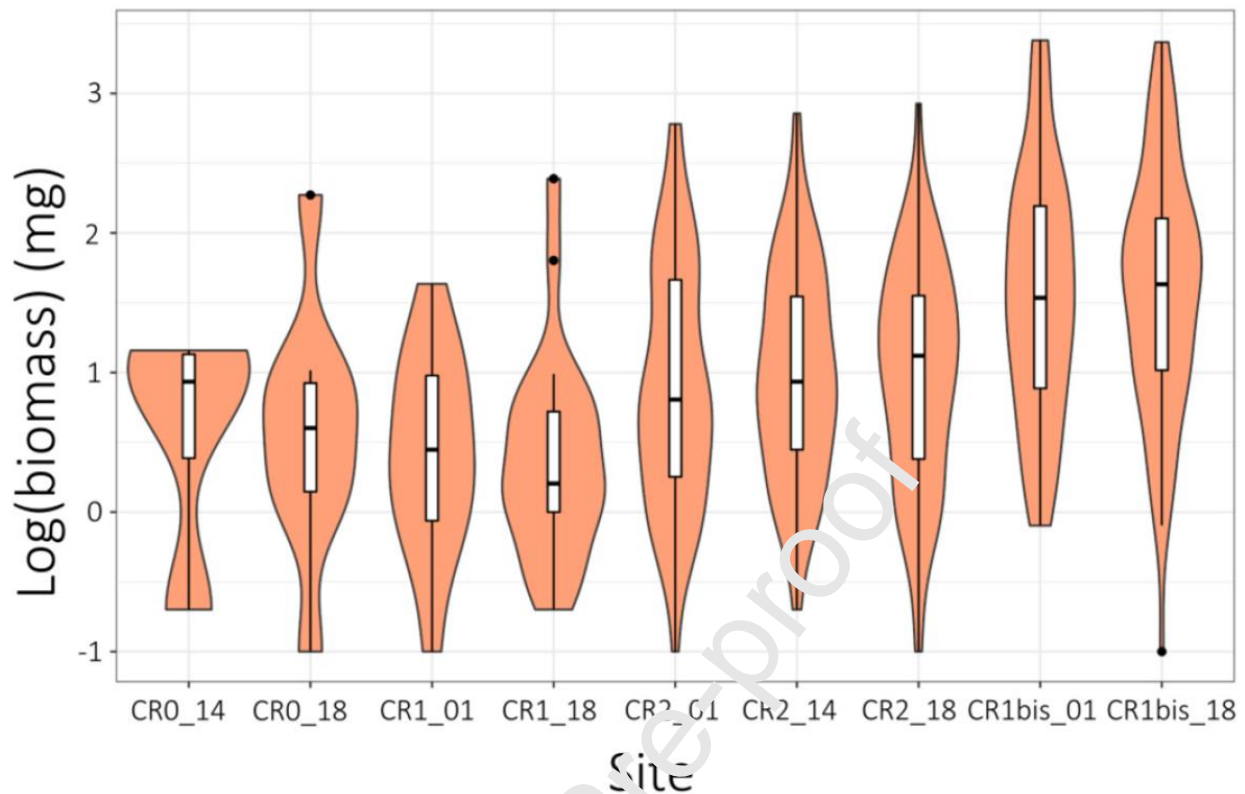


Figure 4: Violin plot of the logarithm of total biomass distribution within communities. Box plots inside show the median (black horizontal thick line), interquartile range between the first and third quartiles (white box), and the two extremes (vertical black whiskers). The black dots represent outliers.

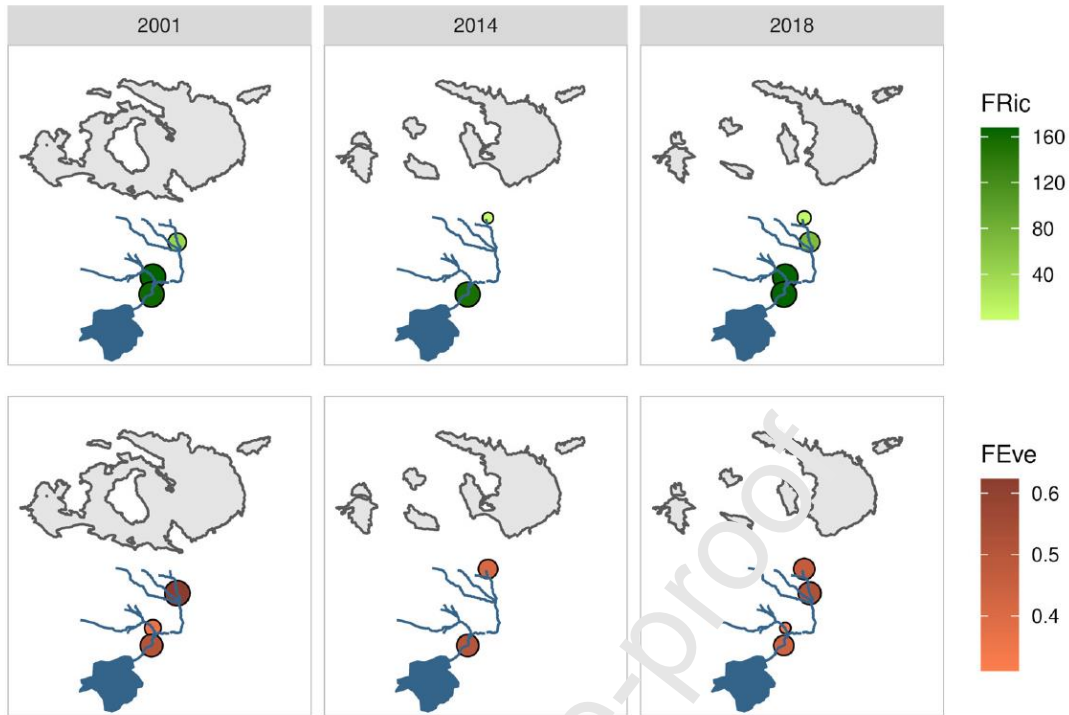


Figure 5: Spatio-temporal evolution of the five functional indexes.

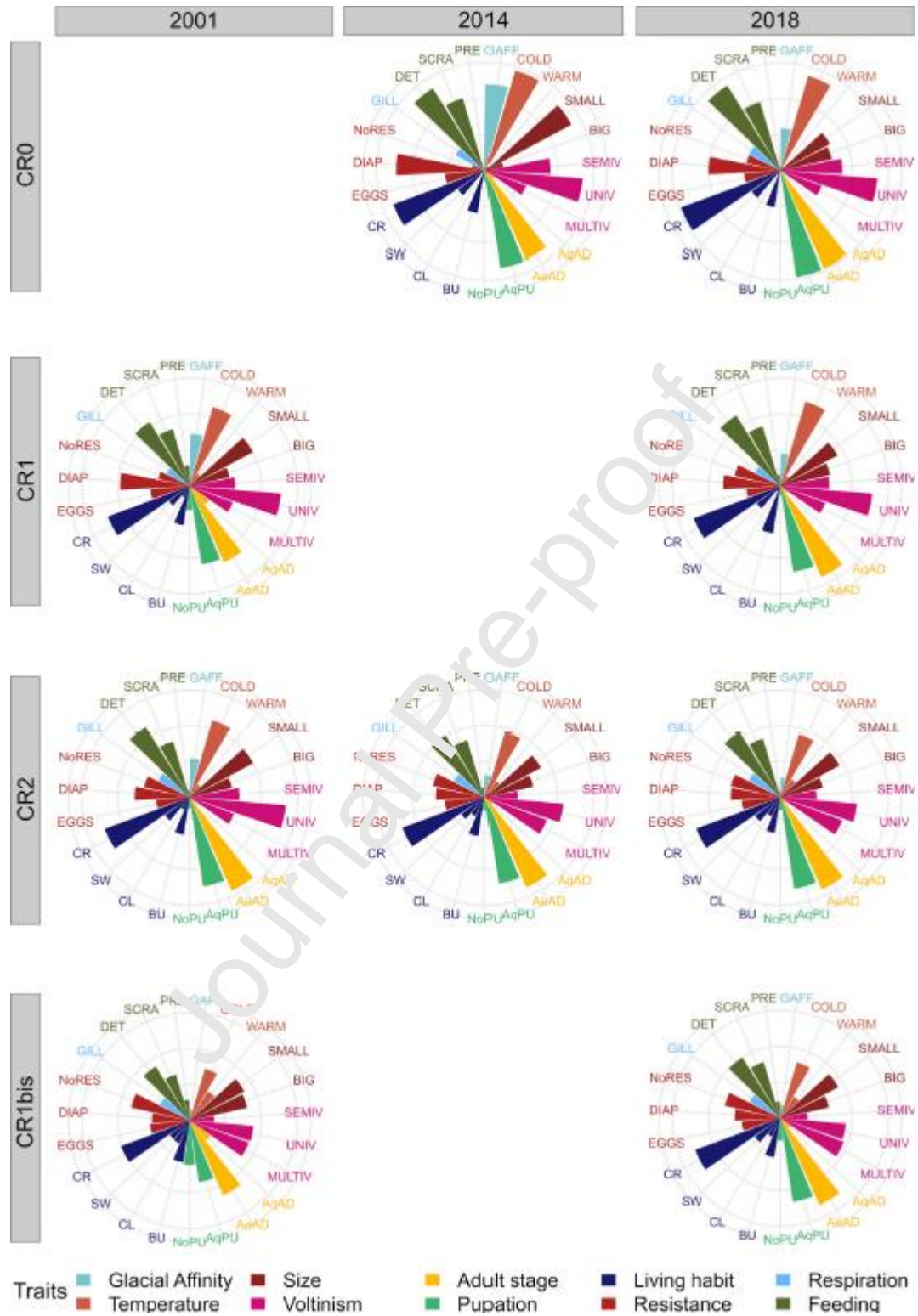


Figure 6: Polar bar chart representing the TCWM (weighted trait values, of the invertebrate community). Values vary from 0 to 3 (third circles). For the sake of clarity, we excluded traits that

do not vary in time and/or space, as shown by the KS analyses (see Supplementary Material).

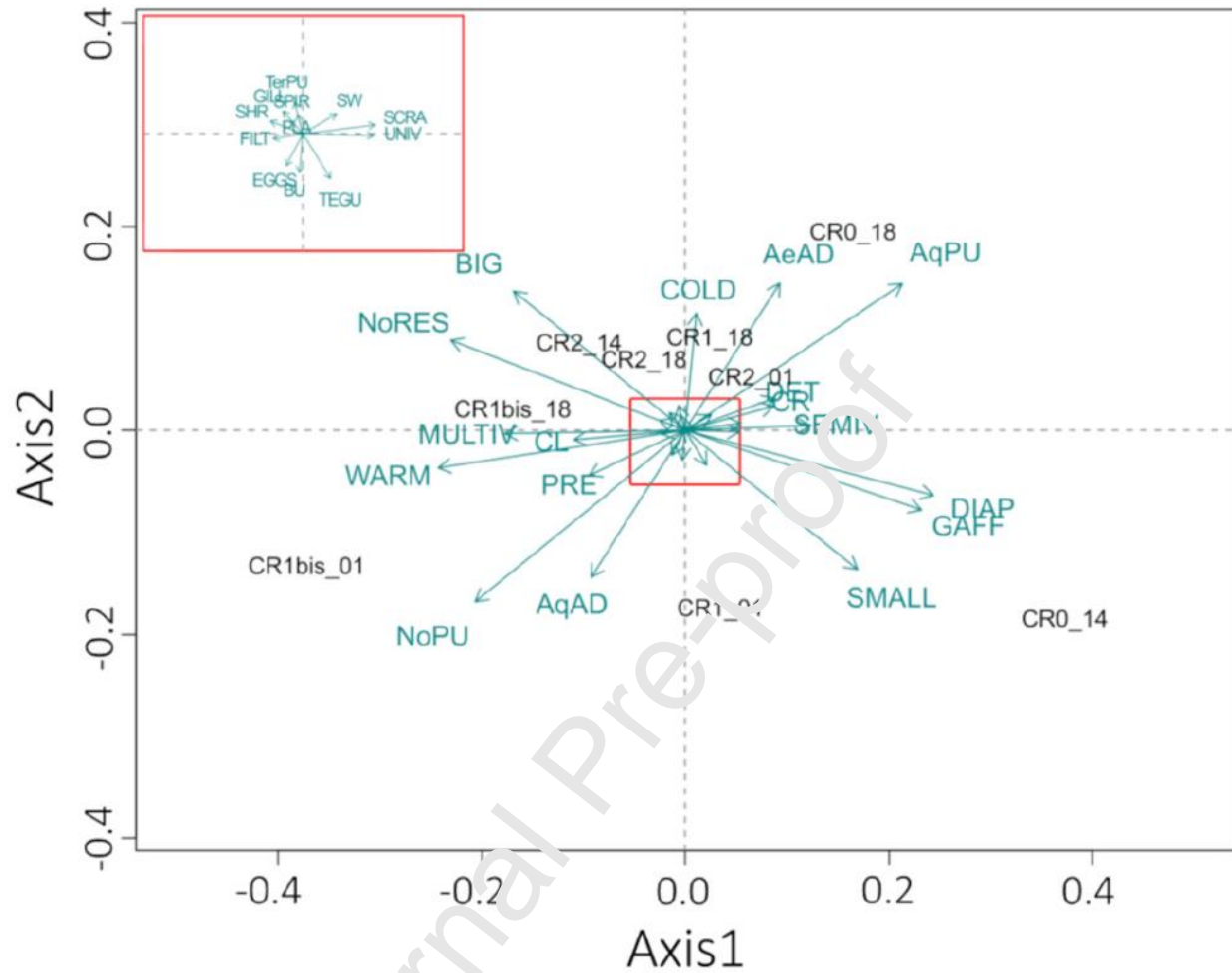


Figure 7: Fuzzy Correspondence analysis performed on TCWM. The figure shows the first two axes, explaining 87.42% of total variability. Total inertia= 0.043.

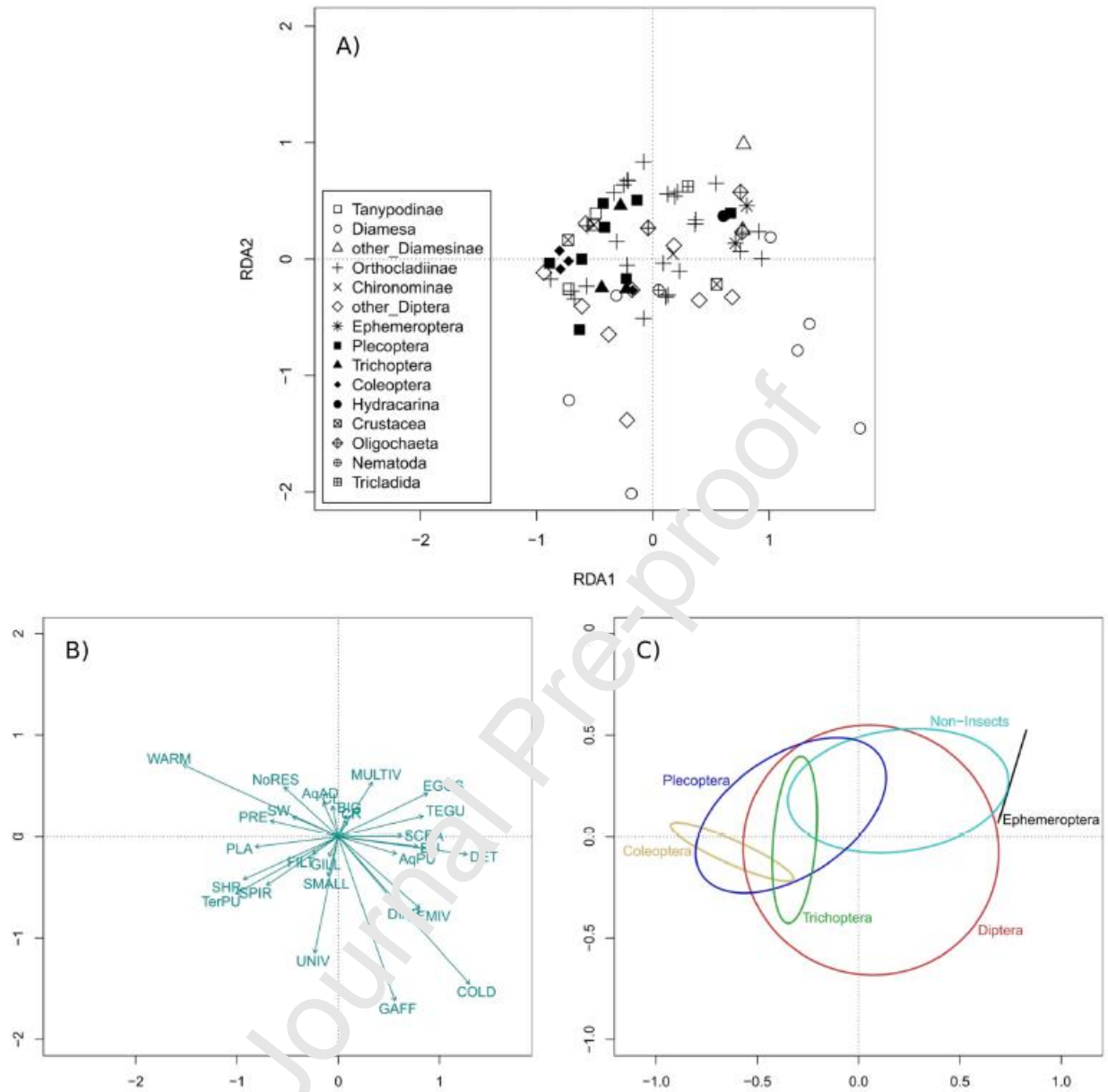


Figure 8: Ordination plot resulting from Redundance Correspondence analysis performed on 73 taxa and 29 biological traits in the plane of the first A) Position of each taxon in relation to the first two constrained axes, explaining 97.7% of the total variability. B) Dominant trait contributions, where length of the vector is related to strength of its contribution to principal coordinate. C) Distribution of taxa grouped into non-insects and insects at the order level.

Author Contributions Statement

Valeria Lencioni: Conceptualisation, writing-review and editing, investigation, field and laboratory activity, supervision;

Elisa Stella: Software, Data curation, Statistical Analysis, Writing; Figure Editing;

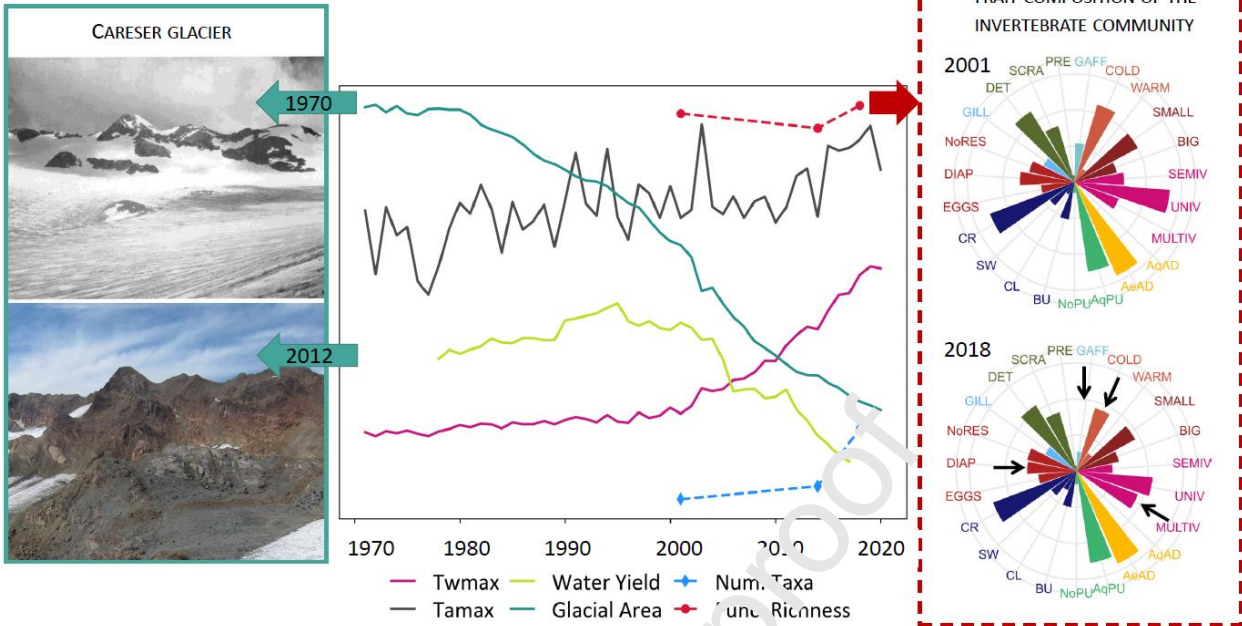
Maria Grazia Zanoni: Software, Data curation, Statistical Analysis, Writing; Figure Editing;

Alberto Bellin: Methodology, Reviewing, Data curation, Statistical Analysis, Supervision.

Declaration of interests

☒ The authors declare that they have no known competing financial interests or personal relationships that could have appeared to influence the work reported in this paper.

☐ The authors declare the following financial interests/personal relationships which may be considered as potential competing interests:



Graphical abstract

Highlights

- Maximum air temperature increased of $1.7\text{ }^{\circ}\text{C}$ since 1980s near the Careser Glacier;
- Almost concurrently, the glacier started to melt, losing losing 74% of its surface in 50 yrs;
- The glacier-fed stream started to warm with a delay of 20 yrs at a rate of $0.2\text{ }^{\circ}\text{C y}^{-1}$;
- Richness and functional diversity increased with a further delay of 13-17 yrs;
- Extinction of *Diamesa steinboeckii* occurred when max summer water temperature $> 6\text{ }^{\circ}\text{C}$.